J Mol Model (2011) 17:151–163
DOI 10.1007/s00894-010-0701-0

ORIGINAL PAPER

Ligand-based and structure-based approaches in identifying ideal pharmacophore against c-Jun N-terminal kinase-3

B. V. S. Suneel Kumar · Rohith Kotla · Revanth Buddiga · Jyoti Roy · Sardar Shamshair Singh · Rambabu Gundla · Muttineni Ravikumar · Jagarlapudi A. R. P. Sarma

Received: 2 September 2009 / Accepted: 28 February 2010 / Published online: 15 April 2010

Abstract Structure and ligand based pharmacophore modeling and docking studies carried out using diversified set of c-Jun N-terminal kinase-3 (JNK3) inhibitors are presented in this paper. Ligand based pharmacophore model (LBPM) was developed for 106 inhibitors of JNK3 using a training set of 21 compounds to reveal structural and chemical features necessary for these molecules to inhibit JNK3. Hypo1 consisted of two hydrogen bond acceptors (HBA), one hydrogen bond donor (HBD), and a hydrophobic (HY) feature with a correlation coefficient (r^2) of 0.950. This pharmacophore model was validated using test set containing 85 inhibitors and had a good r^2 of 0.846. All the molecules were docked using Glide software and interestingly, all the docked conformations showed hydrogen bond interactions with important hinge region amino acids (Gln155 and Met149) and these interactions were compared with Hypo1 features. The results of ligand based pharmacophore model (LBPM) and docking studies are validated each other. The structure based pharmacophore model (SBPM) studies have identified additional features, two hydrogen bond donors and one hydrogen bond acceptor. The combination of these methodologies is useful in designing ideal pharmacophore which provides a powerful tool for the discovery of novel and selective JNK3 inhibitors.

Keywords c-Jun N-terminal kinase · Ligand based-pharmacophore · Docking · Structure based pharmacophore

Introduction

The c-Jun N-terminal kinases (JNKs) are members of the mitogen-activated protein kinase (MAPK) family, which regulate signal transduction in response to environmental stress, and are also known as stress-activated protein kinases. Three distinct genes encoding JNKs have been identified (jnk1, jnk2, and jnk3), and at least 10 different splicing isoforms are believed to exist in mammalian cells [1, 2]. JNK1 and JNK2 have a broad tissue distribution compared to JNK3, which is primarily localized in CNS neurons. However, JNK3 is also found at low levels in heart and testis [3].

Three isoforms of JNK share more than 90% sequence identity and the ATP pocket is almost 98% similar. Although only small differences are present in the primary sequences of the putative binding site, it has been found that the same substrate binds with different affinities to these isoforms. Therefore, it has become a challenging discovery to find novel JNK3 isoform selective ATP competitive inhibitors.

JNK3 appears to play an important role in the brain mediating neurodegenerative processes such as *beta* amyloid processing, Tau phosphorylation and neuronal apoptosis in Alzheimer's disease, and recently, it has also been implicated to have a role in neurotoxicity rodent model of Parkinson's disease [4, 5]. As it mediates neuronal apoptosis, *i.e.*, downstream mechanism of JNK3-mediated apoptosis includes the induction of *Bim* and *Fas* and the mitochondrial release of cytochrome c; inhibiting this isoform makes it a promising therapeutic target for neurodegenerative diseases and stroke [6, 7].

Electronic supplementary material The online version of this article (doi:10.1007/s00894-010-0701-0) contains supplementary material, which is available to authorized users.

B. V. S. S. Kumar · R. Kotla · R. Buddiga · J. Roy · S. S. Singh · R. Gundla · M. Ravikumar (✉) · J. A. R. P. Sarma
bioCampus, GVK Biosciences Private Limited,
S-1, Phase-1, TIE, Balanagar,
Hyderabad 500037, India
e-mail: ravambio@gmail.com

In our present study, we generated ligand and structure based pharmacophore models and also docked selective JNK3 inhibitors into the binding pocket of protein, in order to find the main interactions between the selective inhibitor and receptor at the atomic and amino acid level. In designing this study, we used structure-based and ligand-based pharmacophore approaches with different aims. Structure-based pharmacophore model (SBPM) has the ability to predict the interactions of ligand to the target protein in a very specific way, and also it can reveal the essential features of active site of JNK3 which could contribute for ligand binding.

On the other hand, ligand based quantitative pharmacophore method was used to elucidate the spatial arrangement of structural features of various structurally diverse and potent inhibitors crucial for biological recognition. The ligand-based approach can reveal the common demand of diverse ligands and results in more general pharmacophore models that can be useful for virtual screening of large databases.

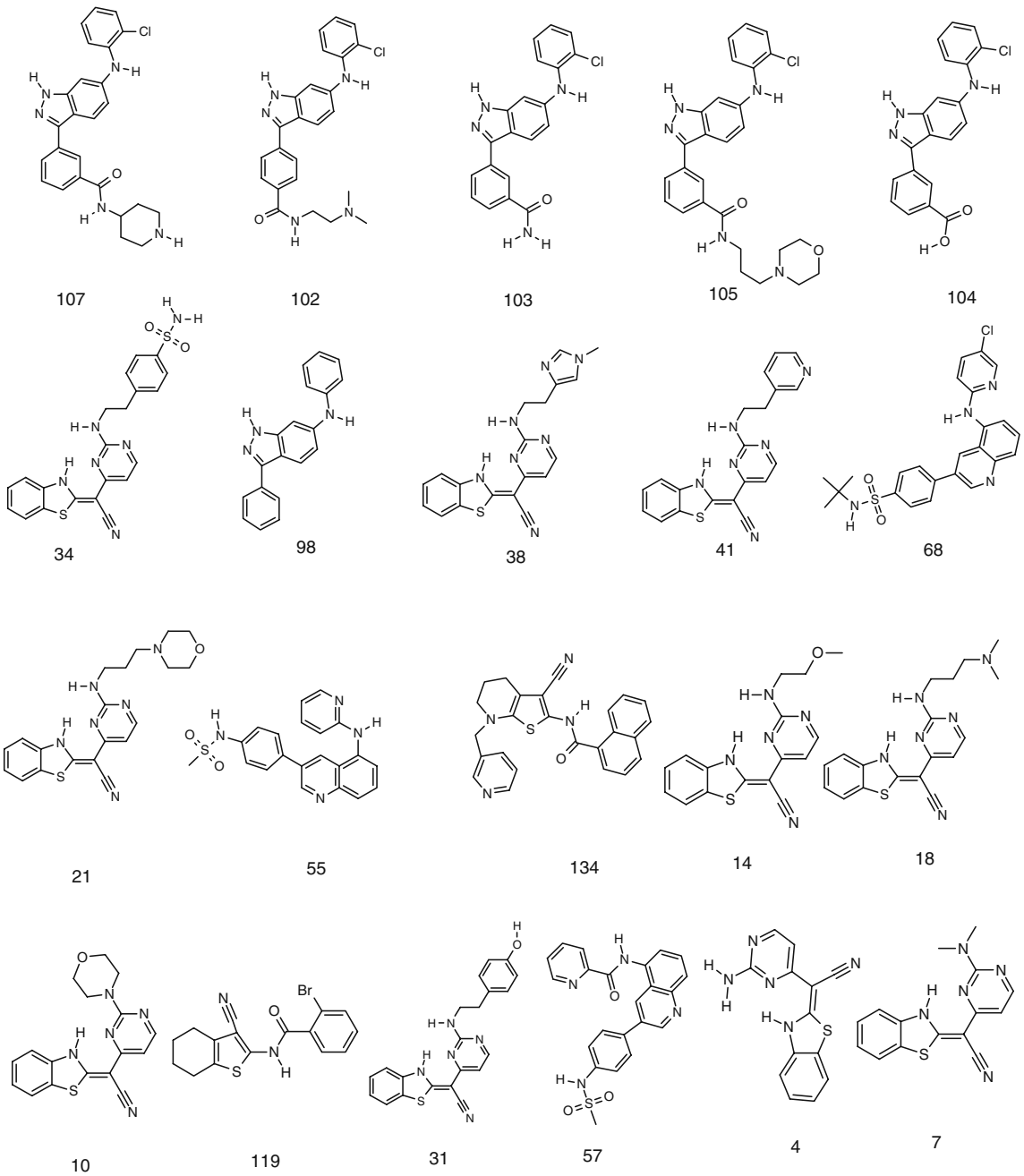

Scheme 1 Chemical structures of the 21 training set molecules applied to HypoGen pharmacophore generation

Materials and methods

Pharmacophore generation

Ligand based pharmacophore studies

Pharmacophore models were generated for inhibitors of JNK3 using Catalyst software package [8]. Catalyst is a relatively new approach that focuses on modeling the drug-receptor interactions using information derived only from the ligand. Chemical-featured quantitative pharmacophore can be generated automatically using the HypoGen algorithm within Catalyst, provided structure-activity relationship data of a well-balanced set of compounds is available.

For the pharmacophore modeling, a set of 106 human JNK3 inhibitors with activity (IC_{50}) spanning over 4 orders of magnitude (from 1.4 nM to 9400 nM) were collected from our database called GOSTAR [9], an online scientific database product. The activity of all the compounds was measured by using human recombinant JNK3. The chemical diversity of these compounds have five different scaffolds (Acetonitrile, 3,5-disubstituted quinolines, 2′-anilino-4,4′-bipyridines, 6-anilinoindazoles and N-(3-cyano-4,5,6,7-tetrahydro-1-benzothien-2-yl)amides). The dataset was divided into a training set (21 compounds, Scheme 1) and test set (85 compounds, Scheme 1 in supporting information), considering both structural diversity and wide coverage of the activity range. The compounds with activity with <100 nM were considered as highly actives (+++), compounds with an activity range between 100–1000 nM were considered as moderate actives (++) and activity of >1000 nM as least actives (+)

All compounds used in the study were subjected to a best method option of conformational search using a Monte Carlo-like algorithm together with poling [10] to generate a maximum of 250 conformers. Our models emphasized a conformational diversity within the constraint of a 20 kcal mol^{-1} energy threshold above the estimated global minimum based on use of the CHARMM force field [11, 12]. All other parameters used were kept at their default settings. The molecules associated with their conformation models were then submitted to Catalyst hypotheses generation.

In hypotheses generation, the structure and activity correlations in the training set were thoroughly examined. HypoGen identifies features that are common to the active compounds but excludes common features for the inactive compounds within conformationally allowable regions of space. Ten hypotheses were generated for every HypoGen run from which the ones with the highest correlation values were chosen. The selected pharmacophore model was validated using cost analysis and test set activity prediction. The best pharmacophore (Hypo 1) having highest correlation coefficient (r), lowest total cost, and lower RMSD value was chosen to estimate the activity of the test set.

Structure-based studies

X-ray crystal structure of JNK3 (PDB ID 2r9s with a resolution of 2.40 Å) was used for structure based pharmacophore and docking studies. For the protein, solvent molecules were deleted and hydrogen atoms were added; and the structures of protein and ligand were combined in a single Macromodel (Schrodinger, Inc.) file. The active site was visually inspected and the appropriate corrections were made for tautomeric states of histidine residues, orientations of hydroxyl groups, and protonation states of basic and acidic residues. The hydrogen atoms were minimized for 3000 steps with Macromodel in the MMFF force field, [13] with all the heavy atoms (non hydrogen) constrained to their original positions. This minimized protein was further used for structure based studies.

Structure based pharmacophore modeling studies (SBPM)

A crystalline complex with a ligand bound to a protein's active site is sufficient information to start the construction

Table 1 Results of pharmacophore hypothesis generated using training set against jnk3-kinase inhibitors

Hypo no	Total cost	Cost-difference[a]	Error cost	RMS	Correlation	Features
1	88.82	50.85	76.59	0.75	0.95	A,A,D,Z
2	89.88	49.79	77.70	0.82	0.94	A,A,D,Z
3	90.22	49.45	77.95	0.83	0.94	A,A,D,Z
4	90.52	49.15	78.24	0.85	0.94	A,A,D,Z
5	90.57	49.10	78.10	0.84	0.94	A,A,D,Z
6	92.61	47.00	80.63	0.97	0.92	A,A,D,Z
7	93.43	46.24	81.41	1.01	0.91	A,A,D,Z
8	93.67	46.00	81.61	1.02	0.91	A,A,D,Z
9	93.97	45.70	82.02	1.04	0.91	A,A,D,Z
10	94.17	45.50	82.20	1.04	0.91	A,A,D,Z

[a] Fixed cost :82.58, Configuration cost 10.822, Null cost 139.676, All cost values are in bits. A=hydrogen bond acceptor, Z=hydrophobic aliphatic, D=hydrogen bond donor

Table 2 Experimental activity and pharmacophore predicted activities of test and training set molecules with docking energies

Compound no	Experimental activity (IC_{50} nM)	Activity scale[b]	Pharmacophore predicted activity	Activity scale	Dock score
107[a]	1.4	+++	1.3	+++	-8.677315
102[a]	1.9	+++	2.3	+++	-8.095716
103[a]	3.3	+++	4.4	+++	-8.964477
105[a]	3.4	+++	8.8	+++	-8.940582
104[a]	5.3	+++	4.3	+++	-8.036478
97	6	+++	69	+++	-8.223112
93	7	+++	21	+++	-8.511295
96	8	+++	87	+++	-7.072015
88	9	+++	27	+++	-8.09064
86	15	+++	21	+++	-8.046127
90	15	+++	21	+++	-7.855313
71	17	+++	27	+++	-6.426854
84	18	+++	95	+++	-6.410482
80	20	+++	53	+++	-7.509982
106	21	+++	8.4	+++	-7.090109
99	30	+++	80	+++	-7.463571
101	32	+++	30	+++	-7.207862
72	32	+++	90	+++	-6.720491
79	32	+++	90	+++	-7.337874
81	33	+++	85	+++	-7.38873
34[a]	41	+++	39	+++	-7.336478
82	44	+++	90	+++	-6.75102
85	44	+++	90	+++	-7.32209
98[a]	48	+++	170	++	-7.240753
38[a]	65	+++	78	+++	-7.168297
33	80	+++	110	++	-5.60253
37	80	+++	110	++	-6.739798
73	108	++	870	++	-6.69444
41[a]	120	++	110	++	-6.727545
61	120	++	130	++	-5.350442
62	140	++	390	++	-6.883023
39	143	++	400	++	-7.776516
43	147	++	200	++	-5.41611
67	150	++	300	++	-6.341756
83	175	++	130	++	-6.278282
114	199	++	200	++	-6.576432
69	200	++	870	++	-6.426222
100	202	++	150	++	-6.109302
89	207	++	120	++	-7.350606
70	240	++	500	++	-5.113889
40	250	++	69	++	-6.822067
68[a]	250	++	500	++	-6.401978
2	250	++	980	++	-4.939269
131	251	++	260	++	-6.220499
132	251	++	400	++	-6.678696
29	273	++	380	++	-5.840753
27	337	++	390	++	-6.701978
28	340	++	190	++	-6.804045
1	350	++	960	++	-6.10139

Table 2 (continued)

Compound no	Experimental activity (IC_{50} nM)	Activity scale[b]	Pharmacophore predicted activity	Activity scale	Dock score
42	397	++	101	++	-5.867777
118	398	++	600	++	-6.344681
21[a]	410	++	250	++	-6.095716
55[a]	440	++	1400	+	-6.568297
36	458	++	440	++	-5.299896
22	473	++	990	++	-5.92061
56	480	++	890	++	-5.855296
63	490	++	850	++	-5.63381
5	500	++	970	++	-5.575856
134[a]	500	++	1000	+	-6.021859
50	510	++	410	++	-6.221048
15	510	++	640	++	-6.025009
75	528	++	170	++	-6.122235
52	530	++	878	++	-5.26269
44	583	++	250	++	-5.92061
45	590	++	960	++	-7.168564
35	600	++	200	++	-5.030789
26	650	++	110	++	-5.727545
74	652	++	910	++	-6.271723
20	660	++	330	++	-6.77133
76	693	++	420	++	-6.030948
19	707	++	1200	+	-5.454647
58	760	++	150	++	-6.830876
17	760	++	1100	++	-6.245291
14[a]	820	++	380	++	-6.13768
6	950	++	1300	+	-4.762383
3	993	++	1900	+	-5.816979
133	1000	+	470	++	-6.051887
115	1000	+	1700	+	-6.045534
46	1000	+	2000	+	-5.915937
12	1300	+	1200	+	-6.00222
49	1300	+	2200	+	-7.216745
24	1324	+	420	++	-5.995814
23	1340	+	160	++	-6.59353
13	1490	+	1100	+	-5.443298
116	1584	+	6900	+	-5.549325
18[a]	1600	+	1100	+	-5.786929
51	1600	+	2200	+	-6.093821
30	1810	+	710	++	-6.238171
129	2511	+	690	+	-5.180092
10[a]	2900	+	1100	+	-5.487808
32	3080	+	560	++	-5.020808
128	3162	+	760	++	-5.695381
130	3162	+	3000	+	-5.42792
117	3162	+	4000	+	-5.406487
119[a]	3200	+	4400	+	-5.518061
31[a]	3500	+	720	++	-5.064477
57[a]	3600	+	2800	+	-5.727545
48	3600	+	4100	+	-6.029609

Table 2 (continued)

Compound no	Experimental activity (IC_{50} nM)	Activity scale[b]	Pharmacophore predicted activity	Activity scale	Dock score
16	3740	+	1100	+	-6.750391
60	6500	+	6500	+	-5.526666
25	6500	+	7400	+	-5.568297
8	6600	+	1200	+	-4.483686
9	6800	+	6000	+	-5.353851
11	7200	+	7400	+	-4.948616
4[a]	7500	+	21000	+	-5.601978
7[a]	9400	+	1400	+	-5.004045

[a] Molecules considered as training set in pharmacophore generation

[b] Activity scale: The compounds with activity with <100 ηM were considered as highly actives (+++), compounds with a activity range of 100-1000 ηM as moderate actives (++) and activity of >1000 ηM as least actives (+)

of a structure-based pharmacophore model. A structure based pharmacophore model (SBPM) was generated using interaction generation module in Discovery Studio 2.0 [14]. Co-crystal N-(tert-butyl)-4-[5-(pyridin-2-ylamino)quinolin- 3-yl]benzenesulfonamide of 2r9s was used to define active site and site sphere defined for 10 A^o to include required aminoacids in the active site. The interaction sphere is generated for the detection and interpretation of crucial interaction patterns between ligand and active site. The crucial interaction patterns were converted into pharmacophore features: hydrophobes, hydrogen bond donors and acceptors along with their direction vectors. For each interaction a cluster of features were generated and the clusters were oriented in different vector directions. The generated crude pharmacophore feature clusters were further refined by carefully selecting each feature from the corresponding cluster, which can establish essential interactions.

Docking studies

All selected inhibitors were docked into the active site of the target protein using Glide (version 8.0, Schrodinger, Inc.) in standard precision mode (Glide SP) [15, 16]. The binding region was defined by a 12 Å _ 12 Å _ 12 Å box centered on the centroid of the co-crystal which is present in the active site of 2r9s, to confine the centroid of the docked ligand. No scaling factors were applied to the Van der Waals radii. Default settings were used for all the remaining parameters. The top 20 poses were generated for each ligand. The docking poses were then energy minimized with Macromodel in the OPLS2001 force field, [17] with flexible ligand and rigid receptor. Best pose was selected on the basis of Glide score and the interactions formed between the ligands and hinge region amino acids.

Results and discussion

Ligand based pharmacophore studies

106 selective inhibitors of JNK3 with activity data spanning over 4 orders of magnitude (from 1.4 nM to 9400 nM) were used for the generation of 3D-pharmacophore models. These compounds were divided into a training set of 21

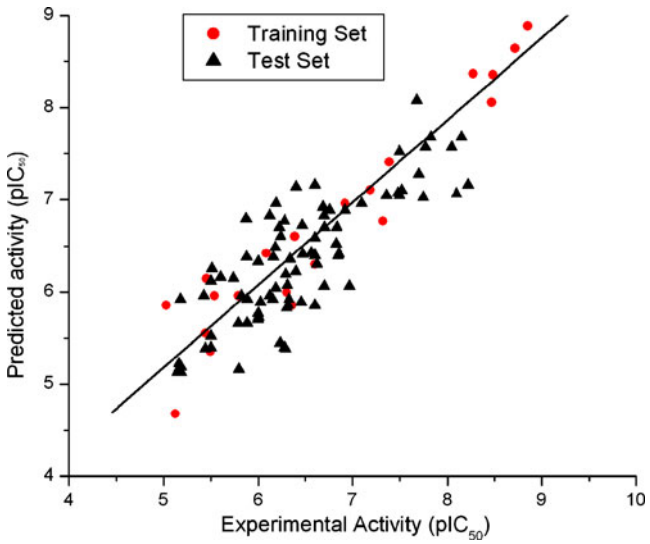

Graph 1 Correlation graph between experimental and Hypo 1-estimated activities of test set

compounds and a representative test set of 85 compounds. HypoGen attempts to construct the simplest hypotheses that best correlates the activities (experimental *vs. predicted)*.

At the end of the run, HypoGen generated 10 pharmacophore models. The Null cost for ten hypotheses was 139.676, the fixed cost of the run was 82.58 and the configuration cost was 10.822. A difference of 57.096 bits obtained between fixed and null costs is a sign of highly predictive nature of hypotheses. All 10 hypotheses generated showed high correlation coefficient between experimental and predicted IC_{50} values, in the range of 0.95 to 0. 91 and moreover, these have a cost difference greater than 45 bits between the cost of each hypothesis and the null cost. This indicates that all the hypotheses have true correlation between 75–90%. The cost values, correlation coefficients (*r*), RMSD, and pharmacophore features are listed in Table 1. The best pharmacophore (Hypo 1) consisted of two H-bond acceptor (HBA), a H-bond donor (HBD), and a hydrophobic aliphatic (HY) feature with a correlation coefficient (*r*) of 0.95, lowest total cost (88.82), and lowest RMSD value (0.75) was chosen to further validate its predictive power by estimating the activity of test set.

The experimental and predicted JNK3 inhibitor activities of the 21 compounds are listed in Table 2. In the training set, among the seven highly active compounds, six were predicted as highly active (+++) and only one compound was predicted as moderately active (++). Out of six moderately active compounds, one compound was predicted as (+++), and the rest were predicted on the target. Out of seven least active compounds, six compounds were predicted as least active (+) and one compound was predicted in moderate active range (++).

For the highly active compound (107) all the features were perfectly mapped to the features of Hypo 1 and had a fit score of 8.45, shown in Fig. 2a. Whereas, for the least active compound (7) only three features of Hypo 1 were mapped properly and had a fit value of 5.42, shown in Fig. 2b. In compound 107, HBA1 feature mapped to the electron rich N atom of indazole ring and HBA2 feature corresponded to the carbonyl group of amide moiety. The HBD feature mapped to the bridge NH group between indazole and piperadine rings. The Hydrophobic group was mapped to the piperadine ring of the compound.

The predictability of Hypo 1 was evaluated by using 85 test set compounds. The generated pharmacophore model has predicted the activity of a diverse dataset of 85 test set compounds with correlation of 0.840 (shown in Graph 1). Pharmacophore mapping of the highest active compound (97) and least active compound (11) on the best hypothesis

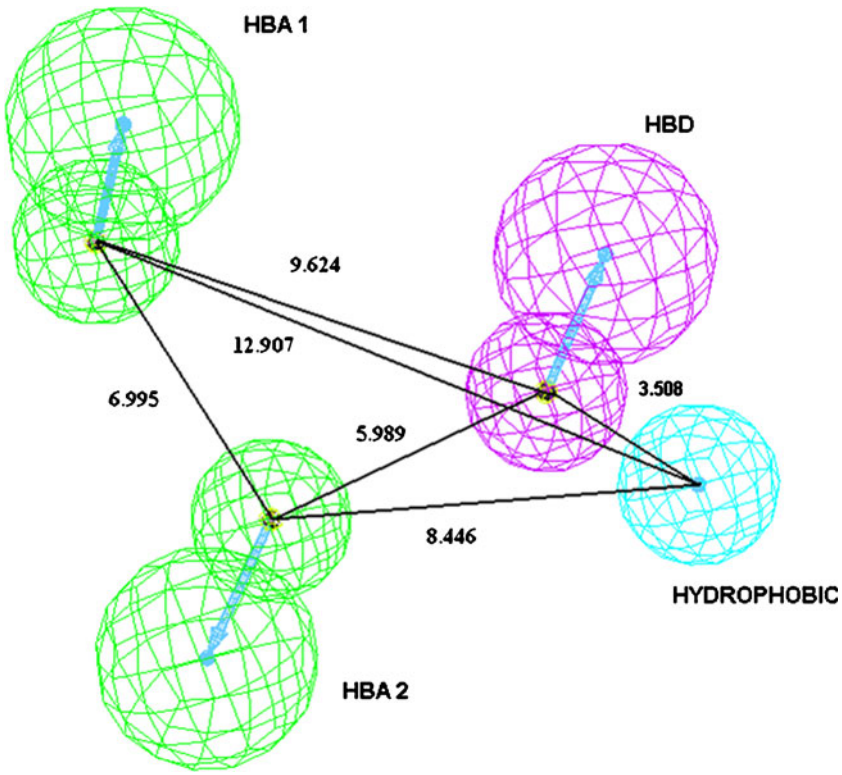

Fig. 1 The best hypothesis model Hypo 1 produced by the HypoGen module in Catalyst 4.11 software. Pharmacophore features are color-coded with green, blue and red contours representing the Hydrogen-bond acceptor feature (A), Hydrophobic feature (Z), hydrogen bond donor respectively. Distance between pharmacophore features are reported in angstroms (Å)

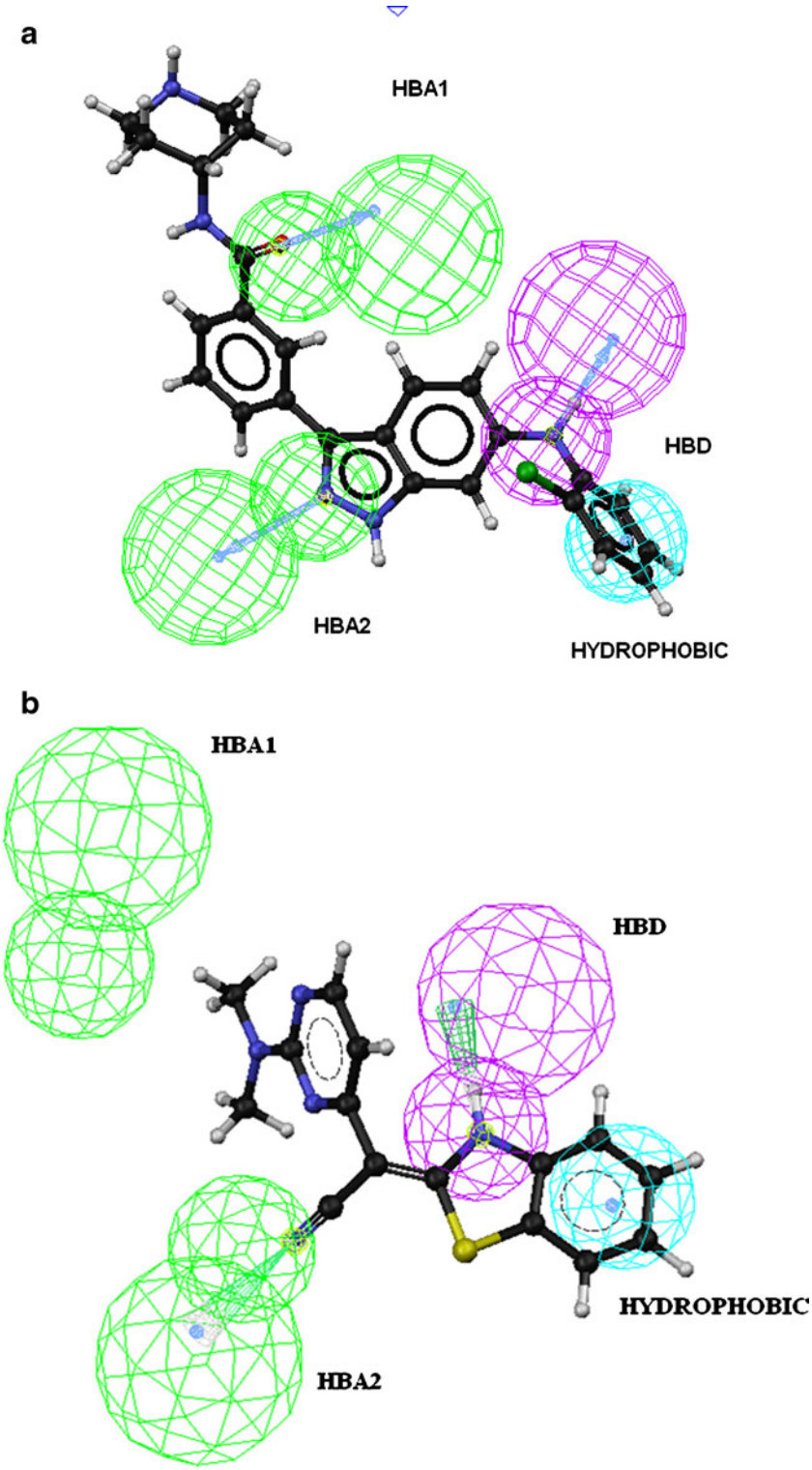

Fig. 2 Pharmacophore mapping of the most active and least active compound (1 from the training set) on the best hypothesis model Hypo 1 (**a**). Pharmacophore mapping of the highest active compound on the best hypothesis model Hypo 1 from the training set model number 107 (**b**) Pharmacophore mapping of the least active compound on the best hypothesis model Hypo 1 from the training set model number 7

model Hypo 1 from the test set are shown in Fig. 1 in supporting information. The compound was predicted in moderate active range (++). The predicted activity of the compounds along with the scale are listed in Table 2. Among the 19 highly active (+++) compounds in the test set, pharmacophore model was able to predict 89.47% of the compounds correctly. Out of 46 compounds present in moderately active (++) range only 90.69% of compounds predicted as (++), but in the least actives (+) 69.56% were predicted as (+) and the remaining were predicted as moderate actives (++). Hence from this analysis, Hypo1 was able to distinguish actives from the inactives.

Ligand-based pharmacophore model (LBPM) was further validated using structure-based studies, *i.e.*, docking and structure based pharmacophore studies, using X-ray crystal structure of JNK3 (PDB entry: 2r9s)

Docking studies

All docking calculations were performed using the "standard precision" (SP) mode of Glide program and with OPLS-AA 2001 force field. All the compounds in the study were docked in the active site of receptor and the binding interactions were calculated. The estimated docking scores (G score) by the algorithm for these compounds are listed in Table 2. These studies provided insight into interactions that may be important for inhibitor activity by comparing docking simulations of each inhibitor in the JNK3 receptor. The electrostatic and few Van der Waals interactions were deemed to be important for binding of the inhibitors. Most of the compounds have hydrogen bond interactions with the hinge region amino acids. Especially highly active compounds are forming at least two hydrogen bond interactions with hinge region amino acids. As shown in the Fig. 3, the docked conformation of highly active compound (107) forms two important hydrogen bond contacts with Gln155 present in the hinge region. The first hydrogen bond is formed by the electron rich nitrogen atom of indazole ring of the compound (N—HN, 2.91 A^o) and the second hydrogen bond is formed by NH of the same indazole ring with side chain carbonyl group of Gln155 (NH—OC, 2.13 A^o).Other crucial hydrogen bond interactions formed between the compound and the receptor are: Met149 backbone carbonyl group with bridge amino group attached between indazole and phenyl rings (NH–OC, 2.82 A^o), carbonyl group of amide group with backbone amine group of Gly71. The compound also forms important hydrophobic interactions Leu206 and Met146.

Amino acids present in JNK3 binding site like Gly71, Ile70, Lys68, Met146, Asn152, Gln155, and Val196 are non-conserved in p38 and ERK2 kinase, while they are conserved in JNK1, JNK2, and JNK3. In hinge region amino acids, Gln155 is the core of the selectivity for JNK3 and this amino acid is not conserved in other map kinases [18, 19].

The ligand based pharmacophore model (LBPM) was able to map all the important interactions which were observed in the docking studies (Fig. 1a). The docking and pharmacophore mapped conformations of compound 107 showed a very small RMSD of 0.846, when they were aligned together. The HBA2 of the pharmacophore model corresponds to a very important interaction with Gln155 of the receptor. The hydrogen bond interaction between ligand and the amino acids (Lys68, Met 149) correlates to the HBA1 and HBD features. The hydrophobic feature appears at the hydrophobic pocket formed by the active site amino acids Met146, Leu206. Thus the generated ligand based pharmacophore model covers all the important interactions of the ligand - receptor complex.

Structure based pharmacophore modeling studies (SBPM)

Pharmacophore and docking studies elucidates the specific interactions between the known ligands and receptor and also narrowing the combination of common features responsible for biological recognition. To improve the flexibility of the features to be selected for inclusion in generating ideal pharmacophore, a structure based phar-

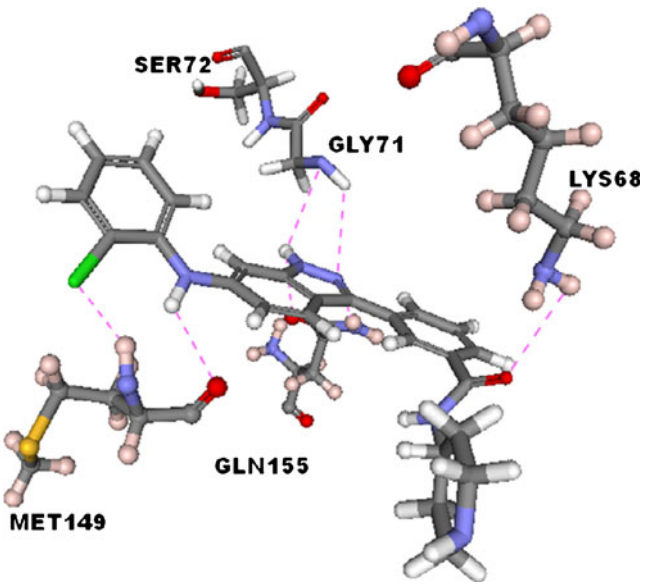

Fig. 3 Docked conformation of the most active compound 107 in the active sites of jnk3. Broken lines represent hydrogen bonds

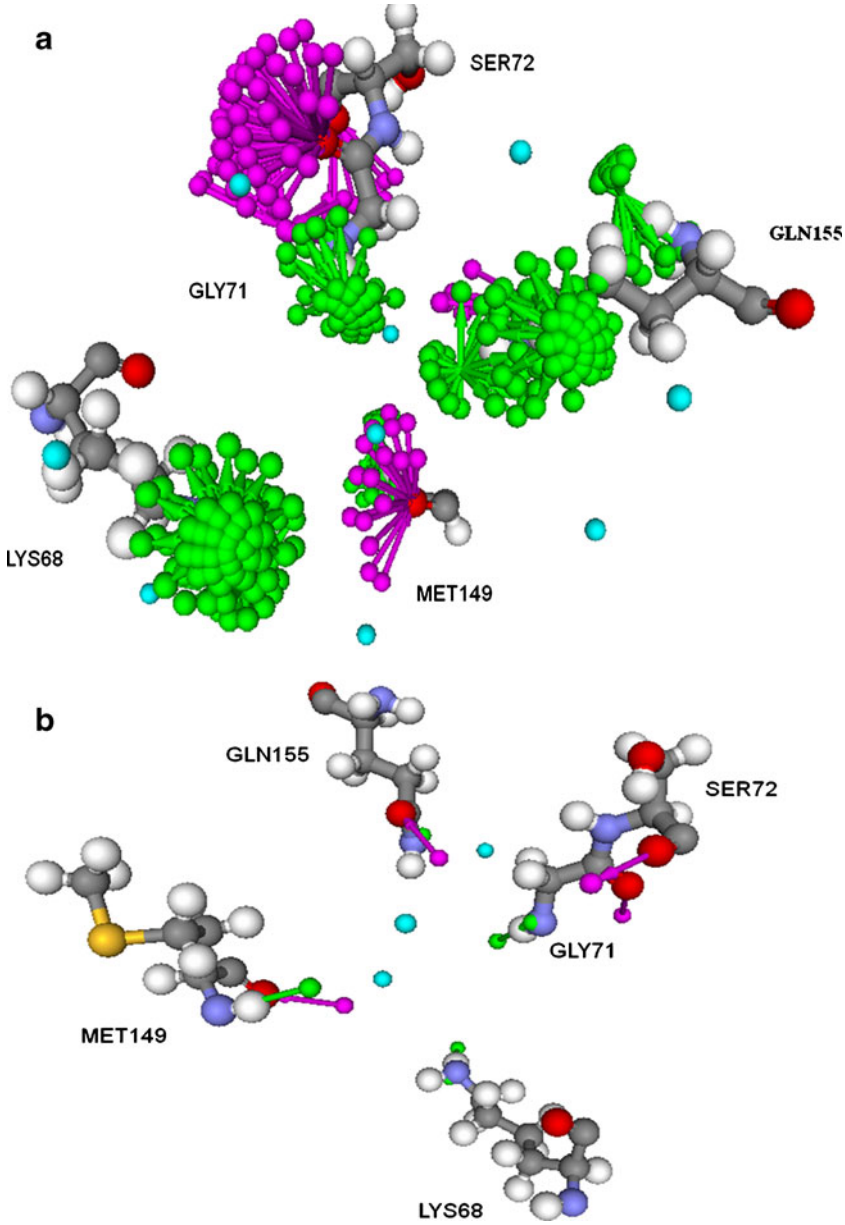

Fig. 4 (**a**) The Structure based pharmacophore clusters produced by the Interaction generation module in Discovery studio. Pharmacophore features are color-coded with green, blue and pink contours representing the Hydrogen-bond acceptor feature (A), Hydrophobic feature (Z), hydrogen bond donor respectively. (**b**). The mapping of selected Structure based pharmacophore from clusters produced by the Interaction generation module in Discovery studio 2.1

macophore approach is the best available option. Structure based pharmacophore *(SBPM)* generates all possible hotspots of the active site that can be converted into best fitting pharmacophore features. Pharmacophore model was generated using interaction generation module in discovery studio. Co-crystal of 2r9s was used as input to define the active site with the help of site sphere around 10 A^{o}. It generated the pharmacophore consisting of the following: hydrophobes, hydrogen bond donors and acceptors along with their direction vectors. Clusters representing various vector features as projected points in different directions are shown in Fig. 4a.

As shown in Fig. 4a, hydrophobic (9), hydrogen bond acceptor (6) and donor clusters (5) were found around Ser72, Gly71, Lys68, Met149, and Gln155. The cluster representing each feature was further refined by carefully selecting each feature from each cluster, which can establish essential interactions (Fig. 4b). The final refined

SBPM consisted of four hydrogen bond acceptor features with Lys68, Gly71, Gln155, Met149 and four hydrogen bond donors with Lys68, Gly71, Ser72, Gln155, Met149 and three hydrophobic features.

On comparison of the SBPM (Fig. 5) with docking interactions, the three hydrogen bond acceptors and two hydrogen bond donors of SBPM are well correlated to the interactions of the compound 107 with Met149, Gln155, Lys68, Met149, Gln155 amino acids of JNK3 obtained in the docking studies. In addition to these docking interactions, SBPM identified one hydrogen bond acceptor interaction with Gly71 and two hydrogen bond donors with Gly71, Ser72.

The features obtained in the LBPM (Hypo1) are well compared to the features of SBPM. As mentioned earlier, the features generated in the LBPM are biased toward the limited chemical diversity of training set but the SBPM is having the advantage of identifying all the hotspots of the active site (ideal pharmacophore). Structure based pharmacophore mapping of the highest active compound 107 is shown in Fig. 2 in supporting information. The additional features present in the SBPM include, two hydrogen bond acceptors, three HBD features, two hydrophobic features.

The features of SBPM, the hydrogen bond acceptor interaction with Gly71 and two hydrogen bond donors with Gly71, Ser72, which are missing in both docking interactions and ligand based pharmacophore studies would definitely contribute to the discovery of novel and more potent leads of JNK3 inhibitors. The process of the generation of the ideal pharmacophore of JNK3 using structure and ligand based pharmacophore models are shown in Fig. 6.

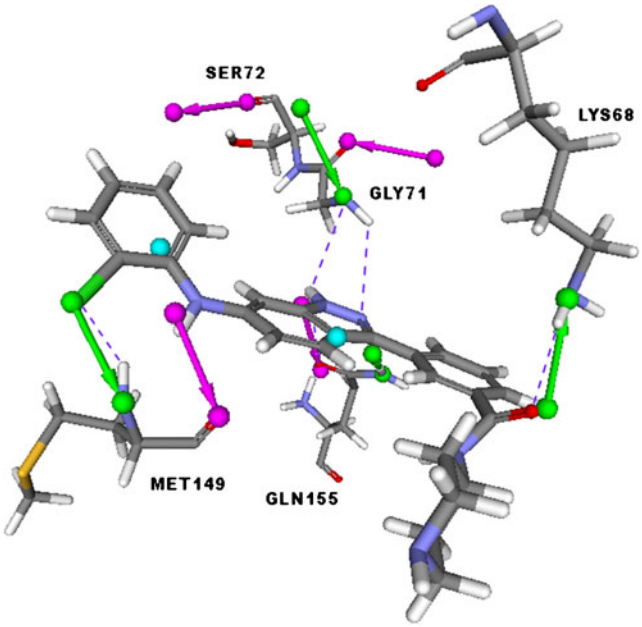

Fig. 5 Comparison of docking interactions and SBPM with best docked conformation of the most active compound 107. Broken lines represent hydrogen bonds. Pharmacophore features are color-coded with green, blue and pink contours representing the Hydrogen-bond acceptor feature (A), Hydrophobic feature (Z), hydrogen bond donor respectively

Virtual screening

The purpose of generating a structure based pharmacophore model was to search the unexplored hot-spots of the JNK-3 active site which can be useful in designing a new chemical space. The feature cluster near Gly71 amino acid in our structure based pharmacophore model was not present in our dataset; hence we chose this feature along with hinge region features as common pharmacophore to search the database (Fig. 3 in supporting information) for finding novel compounds. We found several compounds which have these features from the database. Here we are illustrating one of the compounds obtained from the database in Fig. 3 in supporting information and the interactions are illustrated in Fig. 3b of supporting information and others are in the process of synthesis.

Conclusions

In the present study an attempt was made to evaluate three virtual screening methods, *i.e.*, structure based pharmacophore, ligand based pharmacophore, and docking for the discovery of JNK3 inhibitors. Docking studies [20, 21] revealed important interactions between inhibitor and receptor hinge region amino acids (Gln155 and Met149) and additional hydrogen bonding interactions with Gly71 and Lys68. Observed overall and number of interactions between compound 107 and protein were predicted well by both pharmacophore methods. Also, a structure based pharmacophore model identified hotspots in active site that were not reported in previous JNK3 receptor docking experiments. Structure based pharmacophore generated three new features, not present in ligand based pharmacophore, which would help in discovery of new and potent JNK3 inhibitors.

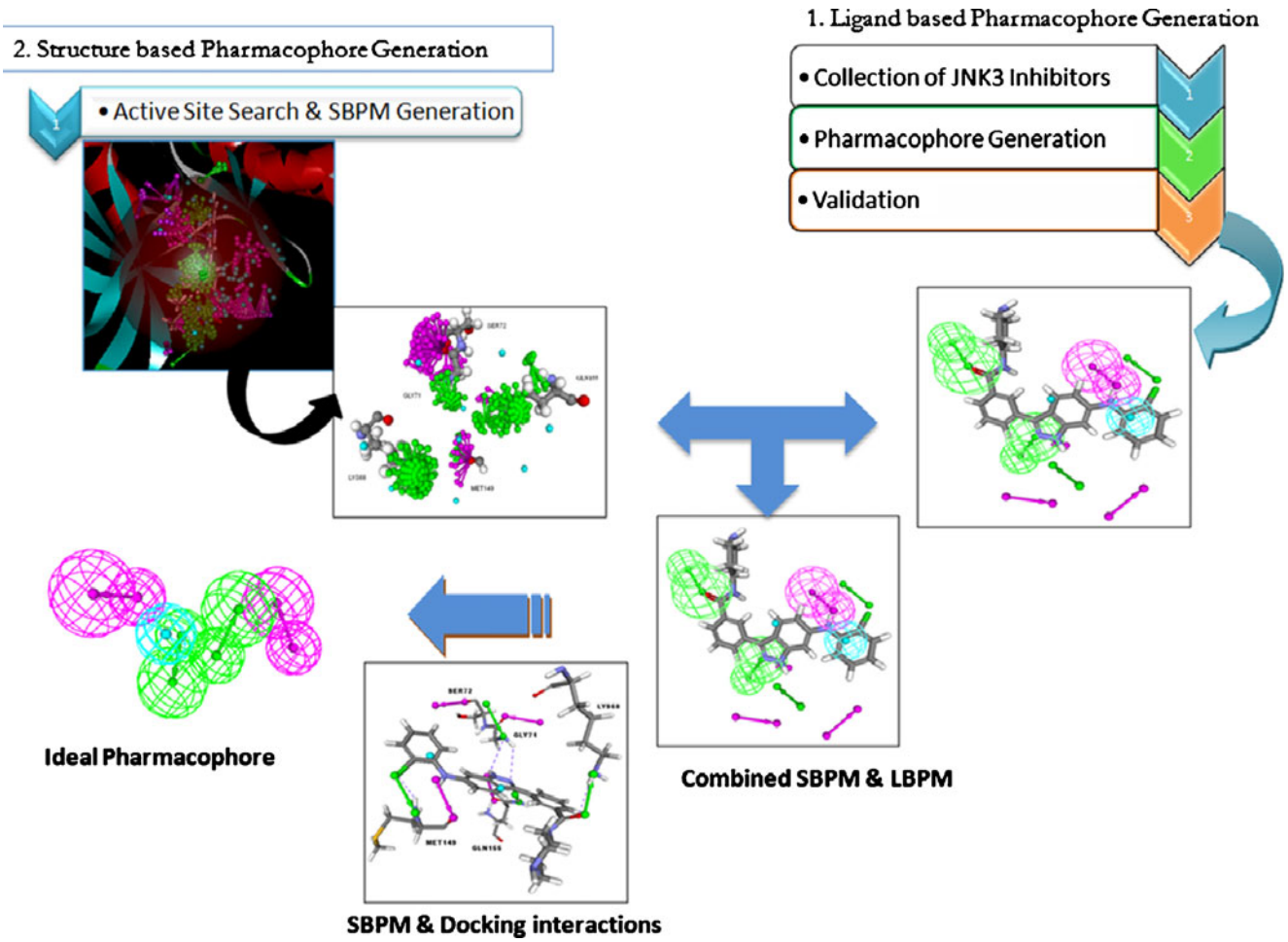

Fig. 6 Flow chart of ideal pharmacophore generation

Acknowledgments The authors would like to thank D.S. Brar, Chairman and G.V. Sanjay Reddy, C.E.O., GVK Biosciences Pvt. Ltd., for their continuous support, S. Rama Devi, T. Sunita, and Raveendra Dayam for their guidance and technical support.

References

1. Gupta S, Barrett T, Whitmarsh AJ, Cavanagh J, Sluss HK, Derijard B, Davis RJ (1996) Selective interaction of JNK protein kinase isoforms with transcription factors. EMBO J 11:2760–2770
2. Mohit AA, Martin JH, Miller CA (1995) p493F12 kinase: a novel MAP kinase expressed in a subset of neurons in the human nervous system. Neuron 1:67–78
3. Resnick L, Fennell M (2004) Targeting JNK3 for the treatment of neurodegenerative disorders. Drug Discov Today 21:932–939
4. Kimberly WT, Zheng JB, Town T, Flavell RA, Selkoe DJ (2005) Physiological regulation of the beta-amyloid precursor protein signaling domain by c-Jun N-terminal kinase JNK3 during neuronal differentiation. J Neurosci 23:5533–5544
5. Kyriakis JM, Avruch J (2001) Mammalian mitogen-activated protein kinase signal transduction pathways activated by stress and inflammation. Physiol Rev 81:807–869
6. Zhang GY, Zhang QG (2005) Agents targeting c-Jun N-terminal kinase pathway as potential neuroprotectants. Expert Opin Invest Drugs 11:1373–1383
7. Kuan CY, Whitmarsh JA, Derek DY, Liao G, Aryn JS (2003) A critical role of neural-specific JNK3 for ischemic apoptosis. Proc Natl Acad Sci 100:15184–15189
8. CATALYST 4.11 Version; Accelrys Inc, San Diego, CA, 2005. http://www.accelrys.com
9. GOSTAR (GVK BIO Online Structure Activity Relationship Database), GVK Biosciences Private Limited, S-1, Phase-1, T.I. E. Hyderabad, A.P, India, 2010. http://www.gostardb.com
10. Smellie A, Teig SL, Towbin P (1995) Poling: promoting conformational variation. J Comput Chem 16:171–187
11. Smellie A, Kahn SD, Teig SL (1995) Analysis of conformational coverage. 1. Validation and estimation of coverage. J Chem Inf Comput Sci 35:285–294
12. Smellie A, Kahn SD, Teig SL (1995) Analysis of conformational coverage. 2. Applications of conformational models. J Chem Inf Comput Sci 35:295–304
13. Halgren TA (1996) Merck molecular force field. I. Basis, form, scope, parameterization, and performance of MMFF94. J Comput Chem 17:490–519
14. Discovery Studio (DS version 2.0, Accelrys Inc., San Diego, CA). http://www.accelrys.com
15. Friesner RA, Banks JL, Murphy RB et al (2004) Glide: a new approach for rapid, accurate docking and scoring. 1.Method and assessment of docking accuracy. J Med Chem 7:1739–1749

16. Halgren TA, Murphy RB, Friesner RA et al (2004) Glide: a new approach for rapid, accurate docking and scoring. 2. Enrichment factors in database screening. J Med Chem 47:1750–1759
17. Jorgensen WL, Maxwell D, Tirado-Rives J (1996) Development and testing of the OPLS all-atom force field on conformational energetics and properties of organic liquids. J Am Chem Soc 118:11225–11236
18. Scapin G, Patel SB, Lisnock J, Becker JW, LoGrasso PV (2003) The structure of JNK3 in complex with small molecule inhibitors - structural basis for potency and selectivity. Chem Biol 10:705–712
19. Boehm JC, Adams JL (2000) New inhibitors of p38 kinase. Expert Opin Ther Pat 13:25–37
20. Shaikh AR, Smael M, Del Carpio CA, Tsuboi H, Koyama M, Endou A, Kubo M, Broclawik E, Miyamoto A (2006) Three-dimensional quantitative structure-activity relationship (3 D-QSAR) and docking studies on (benzothiazole-2-yl) acetonitrile derivatives as c-Jun N-terminal kinase-3 (JNK3) inhibitors. Bioorg Med Chem Lett 16:5917–5925
21. Sharma P, Ghoshal NJ (2006) Exploration of a binding mode of benzothiazol-2-yl acetonitrile pyrimidine core based derivatives as potent c-Jun N-terminal kinase-3 inhibitors and 3D-QSAR analyses. Chem Inf Mode 46:1763–1774